Journal of Sound and Vibration (2000) **237**(1), 67–79
doi:10.1006/jsvi.2000.3026, available online at http://www.idealibrary.com on IDEAL®

EXPERIMENTAL MODAL DENSITIES OF HONEYCOMB SANDWICH PANELS AT HIGH FREQUENCIES

K. RENJI

Structures Group, ISRO Satellite Centre, Bangalore, 560017 India, E-mail: renji@isac.ernet.in

(*Received* 1 *September* 1999, *and in final form* 4 *March* 2000)

The model density of a structure can be experimentally determined from the real part of its driving point admittance. Due to the impedance of the impedance head and the attachment elements, the measured admittance values can be different from the actual driving point admittance, especially at higher frequencies. A correction factor is usually applied to take into account this effect. It is seen that beyond certain frequency, the modal density of honeycomb sandwich panels obtained experimentally using this technique reduces with frequency though the theoretical estimates increase with frequency. This anomaly is investigated in this study. It is found that though the parameter of interest is the real part of the admittance, correction has to be applied considering both real and imaginary parts of the measured admittance. By doing so, it is seen that the experimental modal density values match well with the theoretical results.

1. INTRODUCTION

High-frequency response of a complex structure to broadband acoustic excitation is often evaluated using statistical energy analysis (SEA) developed by Lyon [1] and others. In SEA, one of the important parameters encountered is the modal density of a structural component. The term modal density is defined as the number of resonant modes present in unit frequency band.

Expressions for evaluating the modal densities of commonly used structural elements like beams, plates, shells, honeycomb sandwich panels with isotropic as well as composite face sheets are available in the literature [2–4]. Experimental techniques are also developed for obtaining the modal densities. The modal densities of structural elements are experimentally obtained mainly to validate an expression derived for the modal density and/or to obtain the modal densities of the structural elements that cannot be found theoretically. Mode counting technique, used in many of the earlier works like Erickson [5], gives accurate results only at low frequencies [1]. At higher frequencies, where the parameter modal density is more important, the modes cannot be distinguished due to large modal overlap [1]. Clarkson [6] developed an experimental technique to determine the modal density experimentally which is based on the driving point admittance of the structure. Clarkson and Pope [7] demonstrated this technique by conducting experiments on plates and cylinders. Clarkson and Ranky [3] applied this technique to obtain the modal density of honeycomb sandwich panels with cutouts and stiffeners for which no theoretical expressions exist. Renji *et al.* [4] used this technique to determine the modal density of a composite honeycomb sandwich panel experimentally.

0022-460X/00/410067 + 13 $35.00/0

The modal densities of honeycomb sandwich panels increase with frequency [3, 4] which means that the modal density is higher at higher frequencies. However, Clarkson and Ranky [3] observed an interesting behaviour when the modal density of a honeycomb sandwich panel with isotropic face sheet is determined experimentally using driving point admittance method. At frequencies beyond a certain value, the experimentally obtained modal density decreases with frequency though theoretical results show an increasing trend. This is attributed as due to the vibration of the core cells that occur at high frequencies. Similar behaviour is also reported for honeycomb sandwich panels with orthotropic face sheets [4].

Investigations are carried out on the behaviour of the experimentally obtained modal densities of honeycomb sandwich panels discussed above and the findings are reported in this paper. An improved experimental technique using which the above anomaly is resolved is presented.

2. EXPERIMENTAL TECHNIQUE

Clarkson [6] developed a novel technique to determine the modal density experimentally which is simple and very accurate in the high-frequency range. It was shown that the modal density denoted by $n(f)$, could be obtained from the real part of the driving point admittance using the relation

$$n(f) = 4m\langle \mathrm{Re}(Y)\rangle_a, \tag{1}$$

where m is the mass of the structure. The parameter Y is the driving point admittance, which is the ratio of the Fourier transform of the velocity to the Fourier transform of the driving force. The admittance can be determined using the relation

$$Y = \phi_{fv}/\phi_{ff}, \tag{2}$$

where ϕ_{ff} is the auto-spectral density of the force and ϕ_{fv} is the cross-spectral density between the force and the velocity. To determine the modal density, the driving point admittance should be averaged over different driving point positions. In equation (1), the suffix a represents the driving point location. It is necessary that the structure is having uniform structural properties and it has several modes, more than five, in the frequency band of interest. If the structure has a large number of modes, even single-point admittance can provide the modal density estimates.

Many researchers suggested steps to be taken to improve the application of this technique. Brown [8] discussed about the bias error due to shaker–structure interaction that could be very significant near the natural frequencies. Also, the bias error is sensitive to external noise. He demonstrated that these errors in the measured modal densities could be minimized by measuring the driving point admittance in the following manner:

$$Y = \phi_{sv}/\phi_{sf}, \tag{3}$$

where the suffix s stands for the signal which drives the power amplifier.

For a point excitation, the real part of the driving point admittance should be positive. Clarkson and Pope [7] faced with negative values in the real part of the measured driving point admittance. They used transient excitation to obtain the admittance and this problem occurred for low values of damping. Addition of damping tapes solved the above problem. Use of random excitation helps in avoiding the frequency averaging by properly selecting the frequency bandwidth for the signal analysis [8].

Clarkson and Pope [7] had noticed that the measured driving point admittance values and hence the measured modal densities were influenced by the admittance of the impedance head and the attachment elements. To take into account this effect, Brown and Norton [9] suggested the use of a correction factor as

$$Y_a = Y_m/\{1 - (Y_m/Y_M)\}, \tag{4}$$

where Y_a is the actual admittance and Y_m is the measured admittance. The parameter Y_M is the admittance of the impedance head and the attachment elements, which could be determined by exciting the impedance head and the attaching stud. If M is the mass of the impedance head and the attachment elements, its admittance is given by

$$Y_M = 1/(\mathrm{j}\omega M), \tag{5}$$

where ω is the frequency of excitation in rad/s. The above equation is generally valid for a wide frequency range until the frequency of resonance of the impedance head and the attachment elements.

It is now possible to obtain the modal density experimentally with the help of the basic technique developed by Clarkson [6] along with the help of the various studies carried out for its improvements.

3. DETAILS OF THE PANEL

The mode count of a typical composite honeycomb sandwich panel is obtained experimentally using the technique discussed above. The structural details of the panel considered are given here.

Dimensions	$2{\cdot}15 \times 1{\cdot}80$ m
Area	$3{\cdot}87$ m^2
Thickness of the core	18 mm
Thickness of the face sheet	0·2 mm
Core	3/8–5056–0·0007
Foil thickness of the core	0·018 mm
Cell size	9·54 mm
Density of the core	16 kg/m^3
Shear modulus of the core	$6{\cdot}32 \times 10^7$, $10{\cdot}53 \times 10^7$ N/m^2
Core material	aluminium
Face sheet material	two layers of (0/90) CFRP (carbon fiber-reinforced plastics)
Mass of the panel	13·81 kg

Each CFRP layer has the following properties:

Young's modulus along the fibre direction	30×10^{10} N/m^2
Young's modulus along the transverse direction	$0{\cdot}607 \times 10^{10}$ N/m^2
The major Poisson ratio	0·346
Shear modulus	$0{\cdot}50 \times 10^{10}$ N/m^2

Calculated values of flexural and shear rigidity values are:

D_{11} 5135 N m
D_{22} 5028 N m
D_{12} 69·74 N m

D_{66} 165·6 N m
N 15×10^5 N/m.

For calculating the modal density, the mass of the panel is taken as 10·92 kg. This is obtained by neglecting the lumped masses, as suggested by Clarkson and Ranky [3], such as hinge inserts, hold down inserts and doublers provided at a few locations. At a few locations, local reinforcements are provided.

4. MODAL DENSITY OF THE PANEL

4.1. EXPERIMENTAL RESULTS

In the present experiment, the panel is mounted on a fixture at six locations called hold down points. The fixture in turn is mounted on a seismic mass. The test set-up is shown in Figure 1. Figure 2 shows the locations at which the driving point admittance values are measured. An aluminium block is bonded on the panel and the panel is excited using electro-dynamic shaker connected to the block through a stringer.

The driving point admittance is obtained by measuring the force and acceleration at the driving point. Stationary broadband random excitation is used as the excitation force. From the above signals the cross-spectral densities of velocity and force are calculated. The driving point admittance is then obtained using equation (3). To avoid frequency averaging, as suggested by Brown [8], a low value of resolution, 162·76 Hz, is adapted.

Clarkson and Pope [7] had shown that the mass of the impedance head and the stud between the sensing element and the structure could affect the measured admittance values. Brown and Norton [9] suggested a correction factor for this effect given by equation (4). The measured impedance of the impedance head and the attachment elements used in the present experiment is shown in Figure 3. At 2000 Hz, the impedance is about 237 N s/m. For calculating the actual admittance using equation (4), the value of Y_M averaged over 162·76 Hz bandwidth is used.

The mode count of the panel is derived by multiplying the modal density obtained using equations (1) and (4) by the bandwidth, that is 162·76 Hz. The results thus obtained are given in Table 1 and in Figure 4. In Figure 4, the mode count is given corresponding to the centre frequencies of the bands.

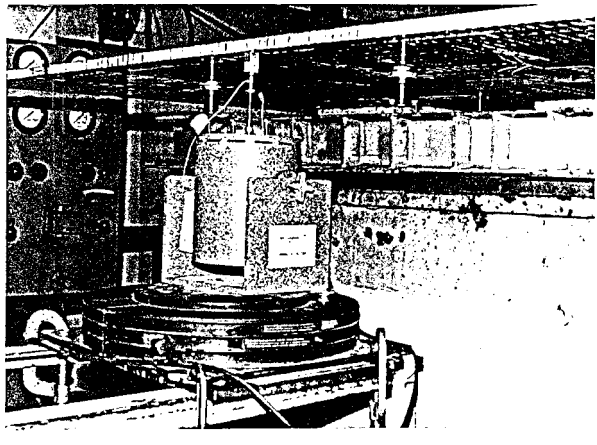

Figure 1. Set-up for the modal density experiment.

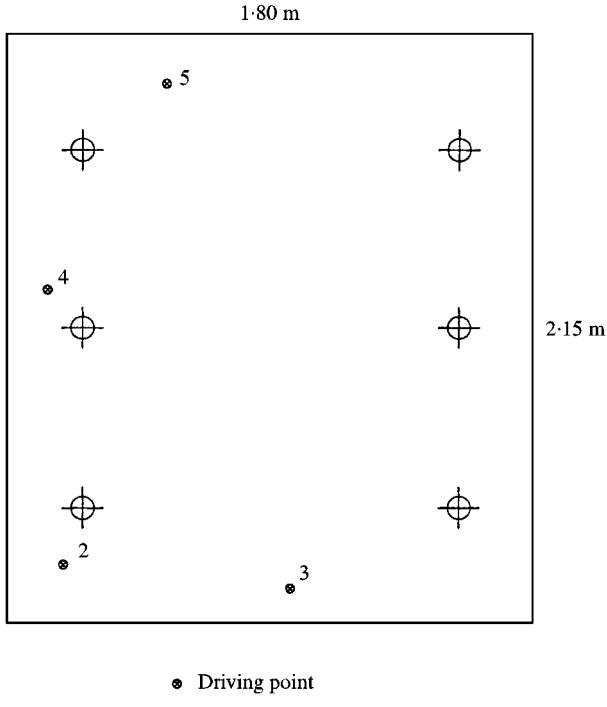

Figure 2. Driving point locations.

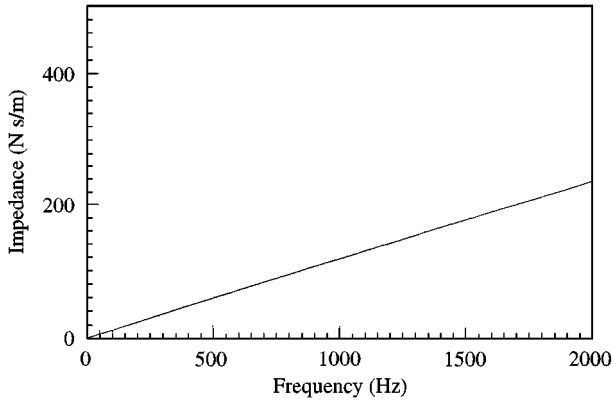

Figure 3. Impedance due to impedance head and the attachment elements.

4.2. THEORETICAL ESTIMATES

The modal density of the honeycomb sandwich panel with composite face sheet, incorporating the transverse shear deformation is given by [4]

$$n(f) = \frac{2ab\rho f}{N} \int_0^{\pi/2} \left\{ \frac{f_2}{f_1} + \frac{1}{f_1} \left[\rho^2 \omega^4 f_2^2 + \frac{4\rho\omega^2 N^2 f_1}{\sqrt{D_{11} D_{22}}} \right]^{-1/2} \left[\rho\omega^2 f_2^2 + 2N^2 \frac{f_1}{\sqrt{D_{11} D_{22}}} \right] \right\} \mathrm{d}\theta. \tag{6}$$

TABLE 1

Mode count of the panel using theory and experiment

Frequency (Hz)	Mode count	
	Theory	Experiment
244–407	10·4	6·1
407–570	11·3	9·6
570–732	12·4	11·1
732–895	13·5	15·7
895–1058	14·6	20·9
1058–1221	15·8	24·2
1221–1384	17·0	21·4
1384–1546	18·3	19·3
1546–1709	19·6	16·4
1709–1872	21·0	16·4
1872–2035	22·3	14·2
2035–2197	23·7	12·5

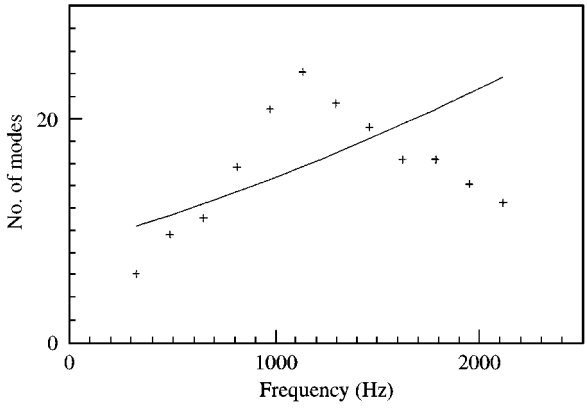

Figure 4. Modal density of a composite honeycomb panel: ——, theory; + , experiment.

In equation (6),

$$f_1(\theta) = 1 - \gamma_1^2 \sin^2(2\theta), \quad f_2(\theta) = (D_{11}/D_{22})^{1/4} \cos^2 \theta + (D_{22}/D_{11})^{1/4} \sin^2 \theta$$

and

$$2\gamma_1^2 = 1 - (D_{12} + 2D_{66})/\sqrt{D_{11}D_{22}}. \tag{7}$$

The parameters D_{11}, D_{22}, D_{12} and D_{66} are the flexural rigidities of the panel and N is the shear rigidity. The panel has dimensions a, b and ρ is its mass per unit area. The shear rigidity of a honeycomb sandwich panel can be estimated using the relation

$$N = G_c t_c \{1 + (t_f/t_c)\}^2. \tag{8}$$

In equation (8), t_f is the thickness of the face sheet, t_c is the thickness of the core and G_c is the shear modulus of the core.

The mode count of the panel used in the experiment is obtained theoretically by using equations (6) and (7). The results of the mode count obtained theoretically as well as experimentally are given in Table 1 and in Figure 4.

4.3. DISCUSSION OF RESULTS

The experimentally obtained mode counts match reasonably well with the theoretical results up to a frequency of 1546 Hz.

From Figure 2, it can be observed that the driving points used in the measurement are not randomly distributed. This is due to some practical difficulties. The panel used is typical of a solar panel of a spacecraft with solar cells bonded to the panel. Therefore, it was possible to excite the structure only at a few selected points. The experimental results are expected to be accurate if randomly located driving points are used.

Beyond 1546 Hz, the measured modal density decreases with frequency though the theoretical results show an increasing trend. Clarkson and Ranky [7] have also reported a similar behavior when they conducted experiments on honeycomb sandwich panels with isotropic face sheets. This is attributed as due to the vibrations of the core cells that occur at high frequencies.

It is to be noted that the three channel technique developed by Brown [8] is not used in the present studies due to some limitations in the measurement of drive signal. The experimental modal density values obtained using the three-channel technique are expected to be only lower than those using the two-channel method [8]. Hence, the above anomaly cannot be resolved by using the three-channel technique.

5. IMPROVED EXPERIMENTAL TECHNIQUE

It was seen previously that beyond certain frequency, the measured modal densities of honeycomb sandwich panels decrease with frequency though the theoretical estimates continue to show an increasing trend. This problem is investigated here.

5.1. THEORY

To determine modal density experimentally, equations (1) and (4) are used. Since only real part of the driving point admittance appears in equation (4), it is natural that only the real part of the driving point admittance is measured. The correction factor is then applied as per equation (4). Hence, if $Y_M = 1/(\mathrm{j}\omega M)$, the equation for Y_a becomes

$$Y_a = \mathrm{Re}(Y_m)/\{1 - \mathrm{j}\omega M\ \mathrm{Re}(Y_m)\}, \tag{9}$$

which will have both real and imaginary parts. Taking the real part of Y_a, we get

$$\mathrm{Re}(Y_a) = \mathrm{Re}(Y_m)/\{1 + [\omega M\ \mathrm{Re}(Y_m)]^2\}. \tag{10}$$

In the experimental results presented previously, equation (10) is used to obtain $\mathrm{Re}(Y_a)$. One can see that the $\mathrm{Re}(Y_a)$ is always smaller than the $\mathrm{Re}(Y_m)$. If $\omega M\ \mathrm{Re}(Y_m)$ is very small compared to unity, the correction factor is approximately unity. At higher frequencies the difference between $\mathrm{Re}(Y_a)$ and $\mathrm{Re}(Y_m)$ is larger. The use of equation (10) to determine the actual admittance assumes that the imaginary part of the measured admittance, denoted by $\mathrm{img}(Y_m)$, is very much negligible.

Let us now obtain the expression for the real part of actual admittance incorporating the imaginary part of the measured admittance also. In that case, it can be shown from equations (4) and (5) that the actual admittance in terms of measured admittance is given by

$$Y_a = \{\mathrm{Re}(Y_m) + \mathrm{j}\,\mathrm{img}(Y_m)\}\{1 + \omega M\,\mathrm{img}(Y_m) + \mathrm{j}\omega M\,\mathrm{Re}(Y_m)\}/\{[1 + \omega M\,\mathrm{img}(Y_m)]^2 + [\omega M\,\mathrm{Re}(Y_m)]^2\}. \tag{11}$$

The real part of the actual admittance now becomes

$$\mathrm{Re}(Y_a) = \mathrm{Re}(Y_m)/\{[1 + \omega M\,\mathrm{img}(Y_m)]^2 + [\omega M\,\mathrm{Re}(Y_m)]^2\}. \tag{12}$$

If $\mathrm{img}(Y_m)$ is negligible, equation (12) reduces to equation (10). For convenience, equation (12) is written as

$$\mathrm{Re}(Y_a) = \mathrm{Re}(Y_m)CF, \tag{13}$$

where the factor CF is given by

$$CF = 1/\{[1 + \omega M\,\mathrm{img}(Y_m)]^2 + [\omega M\,\mathrm{Re}(Y_m)]^2\}. \tag{14}$$

The real part of the actual driving point admittance determined using equation (12) is expected to be accurate compared to what is obtained using equation (10). Though the parameter of interest is the real part of the actual admittance, the use of equation (12) to obtain the real part of the actual admittance necessitates the measurement of both real and imaginary parts of the driving point admittance.

The modal density determined by using equation (12) is termed here as actual experimental modal density and that obtained using equation (10) is termed as apparent experimental modal density. If the $\mathrm{img}(Y_m)$ is + ve, the CF considering the $\mathrm{img}(Y_m)$, is smaller compared to the CF without considering the $\mathrm{img}(Y_m)$. Thus, the actual experimental modal density determined using equation (12), is lower compared to the apparent experimental modal density determined using equation (10). When the $\mathrm{img}(Y_m)$ is −ve, the actual experimental modal density is higher compared to the apparent experimental modal density. If the $\mathrm{img}(Y_m)$ is negligible, that is $\omega M\,\mathrm{img}(Y_m)$ is very small compared to unity, the apparent experimental modal density values are very much close to the actual experimental modal density. The effect of the $\mathrm{img}(Y_m)$ is more significant at higher frequencies.

5.2. RESULTS AND DISCUSSION

The experiments described in section 4 are repeated on the composite honeycomb sandwich panel and both real and imaginary parts of the driving point admittance are measured. The results are shown in Figures 5–8. The real part of the actual admittance is determined using equation (12). The experimentally determined modal densities from these values of $\mathrm{Re}(Y_a)$ are given in Table 2 and Figure 9. The experimental results show good agreement with the estimated modal density values. Hence, by measuring both real and imaginary parts of the driving point admittance and by applying the correction factor as per equation (12), the errors seen in the measured modal densities can be avoided.

The driving point admittance values presented are the frequency-averaged values. For higher order modes, the admittance at a particular frequency is not important and the frequency-averaged admittance values are sufficient. The imaginary part of the actual

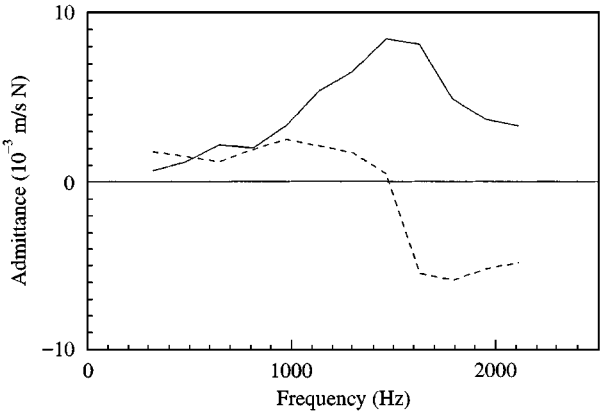

Figure 5. Driving point admittance at location 2: ——, real part; - - -, imaginary part.

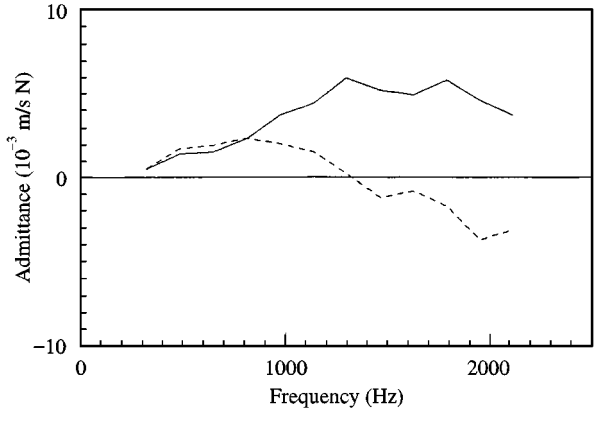

Figure 6. Driving point admittance at location 3: ——, real part; - - -, imaginary part.

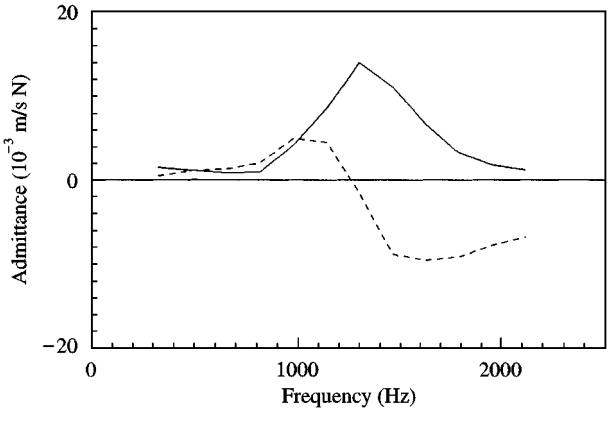

Figure 7. Driving point admittance at location 4: ——, real part; - - -, imaginary part.

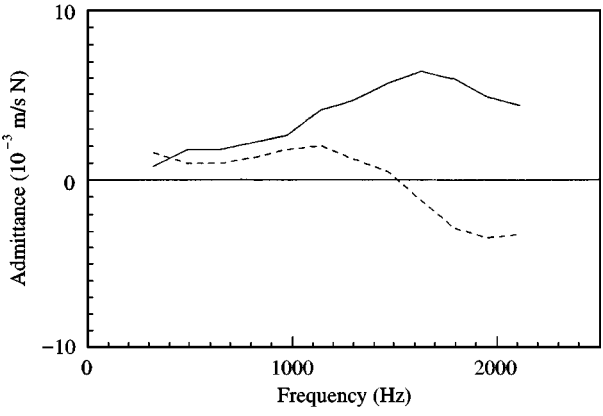

Figure 8. Driving point admittance at location 5: ——, real part; - - -, imaginary part.

TABLE 2

Mode count of a panel using theory and improved experiment

Frequency (Hz)	Mode count	
	Theory	Improved experiment
244–407	10·4	5·7
407–570	11·3	8·3
570–732	12·4	9·2
732–895	13·5	9·4
895–1058	14·6	12·9
1058–1221	15·8	16·5
1221–1384	17·0	19·1
1384–1546	18·3	20·7
1546–1709	19·6	21·9
1709–1872	21·0	23·5
1872–2035	22·3	26·4
2035–2197	23·7	25·9

driving point admittance can be obtained from equation (11) as

$$\mathrm{img}(Y_a) = [\omega M\{\mathrm{Re}^2(Y_m) + \mathrm{img}^2(Y_m)\} + \mathrm{img}(Y_m)][\mathrm{Re}(Y_a)/\mathrm{Re}(Y_m)]. \tag{15}$$

For example, the imaginary part of the actual driving point admittance at location 4, determined using equation (15) is shown in Figure 10. In the case of a thin plate, the imaginary part of the driving point admittance is zero. The imaginary parts seen in the driving point admittance are due to the transverse shear effects of the panel which are significant at higher frequencies, more precisely for higher order modes. It is to be noted that the imaginary parts of the measured admittance values are different from the imaginary parts of the actual admittance values, as shown in Figures 5–8, due to the impedance of the impedance head and the attachment elements. It can be seen from the results that the imaginary part of the driving point admittance can be largely different if corrections are not applied on the measured driving point admittance. By applying the correction factor as

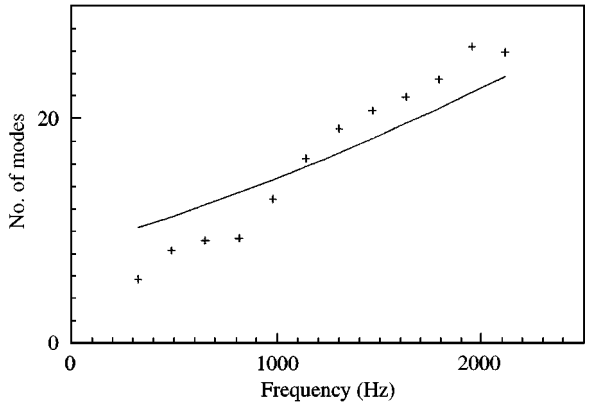

Figure 9. Modal density of a composite honeycomb panel with improved experimental technique: ——, theory; +, experiment.

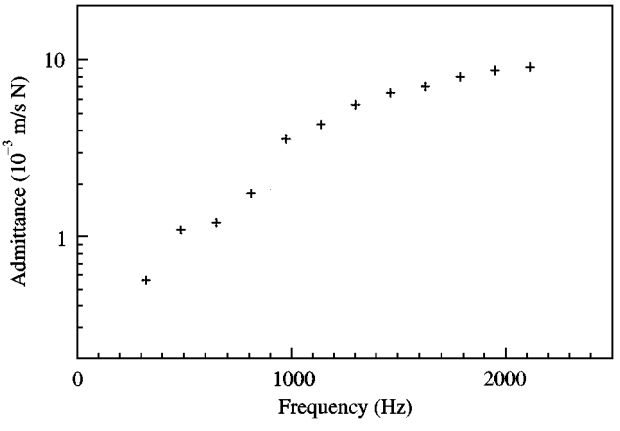

Figure 10. Imaginary part of the actual driving point admittance at location 4.

discussed here, the imaginary parts of the actual driving point admittance can be determined from the measured driving point admittance. Of course, the imaginary part of the actual driving point impedance need not be determined to obtain the modal density.

It is seen from Figure 4 that the experimental modal density when determined using equation (10), that is the apparent experimental modal density, decreases with frequency at frequencies above 1546 Hz. A detailed investigation of the results given in Figures 5–8 shows that at frequencies above 1546 Hz the img(Y_m) is −ve and below this frequency the img(Y_m) is +ve. The Re(Y_m) is always +ve. As discussed earlier, at frequencies where the img(Y_m) is +ve, the apparent experimental modal density will be larger than the actual modal density and at frequencies where the img(Y_m) is −ve, the apparent experimental modal density will be lower than the actual modal density. The frequency at which the img(Y_m) changes its sign from a +ve to a −ve value, there will be a large change in the slope of the apparent experimental modal density. At higher frequencies, the img(Y_m) is −ve and hence the apparent experimental modal density is smaller than the actual experimental modal density. Since deviations of Y_m from Y_a increase with frequency, the

difference between the apparent and the actual experimental modal densities increase with frequency. Hence, beyond the frequency at which the img(Y_m) changes from a +ve to a −ve value, the apparent experimental modal density decreases with the frequency.

It remains now to investigate on the frequency at which the img(Y_m) changes from a +ve to a −ve value. This frequency is seen to be dependent on the properties of the honeycomb sandwich panel. The core used is 3/8-5056-0.0007. The fundamental mode of the core cell is estimated to be 1520 Hz. The frequency calculated is the first mode of bending vibration of the cell wall for simply supported boundaries. One can see that around this frequency the img(Y_m) changes its sign. Hence, it can be concluded that img(Y_m) changes its sign at the frequency of the fundamental mode of vibration of the core cell walls. Clarkson and Ranky [3] reported that the measured experimental modal density of a honeycomb sandwich panel decreases beyond a certain frequency. In their results this frequency is about 4500 Hz. The first mode of vibration of the core cell used in their experiment is calculated and found to be 4616 Hz. The above results clearly show that the anomaly in the measured modal densities occurs beyond the frequency of the vibration of the core cells and hence this will occur for all honeycomb sandwich panels.

6. CONCLUSIONS

When the modal density is obtained experimentally from the real part of the driving point admittance, corrections for the impedance of the impedance head and the attachment elements have to be incorporated. While arriving at the correction factors, both the real and imaginary parts of the measured admittance have to be taken into consideration though the parameter of interest is the real part of the admittance. This is particularly important for honeycomb sandwich panels. For such panels if the imaginary part of the measured driving point admittance is not considered, the experimentally determined modal density will be in large error. In such cases, that is without considering the imaginary part of the driving point admittance, beyond the frequency of the fundamental mode of the core cells walls, the experimentally determined modal density decreases with frequency though the theoretical estimates continue to increase. The imaginary part of the measured driving point admittance can be largely different from the actual driving point admittance due to the impedance of the impedance head and the attachment elements. To determine the imaginary part of the actual driving point admittance, correction factors need be applied on the measured driving point admittance.

ACKNOWLEDGMENT

The author wishes to thank Dr P.S. Nair, Group Director, Structures, ISRO Satellite Centre for his valuable suggestions.

REFERENCES

1. R. H. Lyon 1975 *Statistical Energy Analysis of Dynamical Systems*: *Theory and Applications*. Cambridge, MA: MIT Press.
2. F. D. Hart and K. C. Shah 1971 *NASA CR*-1773. Compendium of modal densities.
3. B. L. Clarkson and M. F. Ranky 1983 *Journal of Sound and Vibration* **91**, 103–118. Modal density of honeycomb plates.
4. K. Renji, P. S. Nair and S. Narayanan 1996 *Journal of Sound and Vibration* **195**, 687–699. Modal density of composite honeycomb sandwich panels.

5. L. L. ERICKSON 1969 *The Shock and Vibration Bulletin* **39**, 1–16. Modal densities of sandwich panels: theory and experiment.
6. B. L. CLARKSON 1981 *Journal of Sound and Vibration* **77**, 583–584. The derivation of modal densities from point impedances.
7. B. L. CLARKSON and R. J. POPE 1981 *Journal of Sound and Vibration* **77**, 535–549. Experimental determination of modal densities and loss factors of flat plates and cylinders.
8. K. T. BROWN 1984 *Journal of Sound and Vibration* **96**, 127–132. Measurement of modal density: an improved technique for use on lightly damped structures.
9. K. T. BROWN and M. P. NORTON 1985 *Journal of Sound and Vibration* **102**, 588–594. Some comments on the experimental determination of modal densities and loss factors for statistical energy analysis applications.

APPENDIX: NOMENCLATURE

Symbols not listed here are used only at specific places and are explained wherever they occur.

a,b	dimensions of a panel
$D_{11}, D_{22}, D_{12}, D_{66}$	flexural rigidity values of a laminate
f	frequency, in Hz
G_c	shear modulus of the core
$\mathrm{img}(x)$	imaginary part of the variable x
M	mass of impedance head and the attachment elements
m	mass of a panel
N	shear rigidity of a panel
$n(f)$	number of modes per Hz
$\mathrm{Re}(x)$	real part of x
t_c	thickness of the core
t_f	thickness of the face sheet
Y	driving point admittance
Y_a	actual driving point admittance
Y_M	admittance of the impedance head and attachment elements
Y_m	measured driving point admittance
ϕ_{xx}	spectral density of the random process x
ϕ_{xy}	cross-spectral density between the random processes x and y
ω	circular frequency, in rad/s
ρ	mass per unit area
$\langle\rangle_x$	average over the domain x